UV light phototransduction activates transient receptor potential A1 ion channels in human melanocytes

Nicholas W. Bellono, Laura G. Kammel, Anita L. Zimmerman, and Elena Oancea[1]

Department of Molecular Pharmacology, Physiology, and Biotechnology, Brown University, Providence, RI 02912

Edited* by David E. Clapham, Howard Hughes Medical Institute, Children's Hospital Boston, Boston, MA, and approved December 26, 2012 (received for review September 10, 2012)

Human skin is constantly exposed to solar ultraviolet radiation (UVR), the most prevalent environmental carcinogen. Humans have the unique ability among mammals to respond to UVR by increasing their skin pigmentation, a protective process driven by melanin synthesis in epidermal melanocytes. The molecular mechanisms used by melanocytes to detect and respond to long-wavelength UVR (UVA) are not well understood. We recently identified a UVA phototransduction pathway in melanocytes that is mediated by G protein-coupled receptors and leads to rapid calcium mobilization. Here we report that in human epidermal melanocytes physiological doses of UVR activate a retinal-dependent current mediated by transient receptor potential A1 (TRPA1) ion channels. The TRPA1 photocurrent is UVA-specific and requires G protein and phospholipase C signaling, thus contributing to UVA-induced calcium responses to mediate downstream cellular effects and providing evidence for TRPA1 function in mammalian phototransduction. Remarkably, TRPA1 activation is required for the UVR-induced and retinal-dependent early increase in cellular melanin. Our results show that TRPA1 is essential for a unique extraocular phototransduction pathway in human melanocytes that is activated by physiological doses of UVR and results in early melanin synthesis.

Skin provides a protective barrier to the external environment. Solar ultraviolet radiation (UVR), a prevalent risk factor for skin cancer, evokes a unique response in human skin that leads to increased pigmentation (1). UVR-induced pigmentation is a protective response mediated by melanin synthesis in human epidermal melanocytes (HEMs) to shield DNA from UVR-induced damage (2). While the mechanism by which short-wavelength UVR (UVB) results in increased pigmentation has been characterized (1), very little is known about phototransduction of long-wavelength UVR (UVA) in human skin.

Transient receptor potential (TRP) ion channels were first characterized in *Drosophila* phototransduction as calcium- (Ca^{2+}) permeable ion channels, essential for light activation of rhabdomeric photoreceptors (3–5). More recently, members of the TRP family have been implicated in a wide range of sensory functions, including photosensation, chemosensation, thermosensation, and nociception (6, 7). In mammalian phototransduction, TRPC channels mediate a light-sensitive current in intrinsically photoreceptive retinal ganglion cells, which are responsible for non-image-forming visual processes in the human retina (8–11). TRP channels are also expressed in the epidermis and are activated by noxious compounds, acidic pH, and temperature (12–14).

We recently characterized a retinal-dependent, UVA-activated pathway in HEMs that is mediated by G protein activation and leads to a rapid Ca^{2+} release from internal stores and Ca^{2+}-dependent early melanin production (15). Here we show that UVA phototransduction in human melanocytes activates a TRP channel, subfamily A member 1 (TRPA1), leading to a retinal-dependent current and a rapid Ca^{2+} influx. TRPA1 activation is G protein and phospholipase C (PLC)-dependent and causes a Ca^{2+} influx necessary for UVA-induced early melanogenesis. Our results demonstrate that UVR doses corresponding to seconds to minutes of sun exposure activate TRPA1 channels in melanocytes to increase melanin production, providing evidence for TRPA1 function in mammalian extraocular phototransduction and melanin synthesis.

Results and Discussion

UVR Activates a Retinal-Dependent Current in HEMs. Using a setup that allows for simultaneous electrophysiological recordings and exposure of cultured cells to UVR, we sought to investigate if ion channels present in the plasma membrane of human melanocytes are activated by physiological UVR doses. We exposed cultured HEMs to radiation with spectral characteristics similar to solar UVR and doses equivalent to seconds to minutes of full sun exposure (15), and measured ionic fluxes across the plasma membrane using whole-cell patch-clamp recordings. Exposure to 240 mJ/cm^2 UVR (equivalent to 240 s of full sun exposure) evoked a significant increase in current at +80 mV only when HEMs were preincubated with retinal (Fig. 1*A*), the chromophore required for light activation of opsin G protein-coupled receptors (GPCRs) (16). This current was independent of the form of retinal used: the UVR-induced increase in current at +80 mV normalized to capacitance values [I_{UVR} (pA/pF)] was similar following preincubation with 9-*cis* [an 11-*cis*-retinal analog, 12 μM (17)], or all-*trans* retinal (12 μM) (Fig. 1*B*). To further characterize this photocurrent, we used a voltage-step protocol to determine the current density as a function of voltage in the presence and absence of *trans*- or *cis*-retinal (Fig. 1*C*). We found that the UVR photocurrent is outwardly rectifying and has a reversal potential near 0 mV, a current-voltage relationship consistent with many TRP channels (18).

The ability of both forms of retinal to evoke a photocurrent might be because of the conversion of all-*trans* to *cis*-retinal in melanocytes, possibly using the retinoid isomerase RPE65, which is expressed in skin (19) and catalyzes the conversion of *trans*-retinal to the *cis*- conformation, as in the visual cycle in mammalian rod and cone cells (10). Alternatively, the pigment mediating UVR phototransduction in HEMs could drive signaling using either *cis*- or *trans*-retinal, similar to the bistable opsins required for nonvisual phototransduction in the mammalian retina or invertebrate phototransduction (10, 20).

UVR-Induced Current Is Activated by Physiological Doses of UVR. To determine the UVR dose-dependence of the retinal-dependent photocurrent, we measured current amplitudes in response to UVR doses between 40 and 440 mJ/cm^2 (corresponding to 40–440 s of exposure to full sun) (Fig. 1 *D* and *E*), resulting from exposure to 20 mW/cm^2 for increasing time intervals (2–22 s) (Fig. 1*D*). UVR-activated current increased in a dose-dependent manner, required a minimum dose of 140 mJ/cm^2, and reached saturating amplitude at 340 mJ/cm^2 (Fig. 1*E*), which was blocked in the presence of ruthenium red (RR, 10 μM), a broad TRP channel inhibitor

Author contributions: N.W.B., A.L.Z., and E.O. designed research; N.W.B. and L.G.K. performed research; E.O. contributed new reagents/analytic tools; N.W.B. analyzed data; and N.W.B. and E.O. wrote the paper.

The authors declare no conflict of interest.

*This Direct Submission article had a prearranged editor.

[1]To whom correspondence should be addressed. E-mail: elena_oancea@brown.edu.

This article contains supporting information online at www.pnas.org/lookup/suppl/doi:10.1073/pnas.1215555110/-/DCSupplemental.

Downloaded at Palestinian Territory, occupied on December 18, 2021

www.manaraa.com

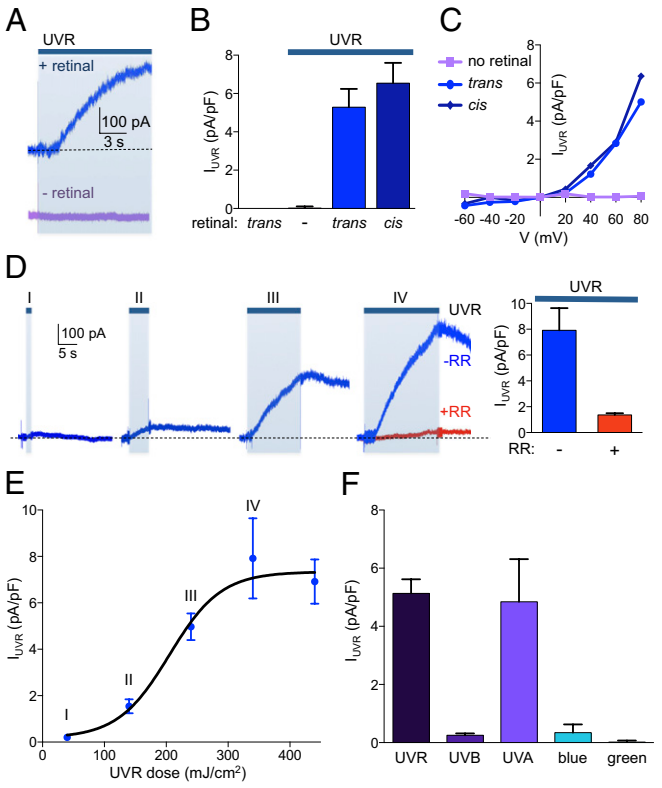

Fig. 1. UVR activates a retinal- and dose-dependent UVA-specific current in HEMs. (*A*) UVR activates a retinal-dependent, outwardly rectifying current in HEMs that has a reversal potential near 0 mV. Whole-cell current amplitude at +80 mV in a representative HEM stimulated with 240 mJ/cm^2 UVR (shaded box, 12 s of 20 mW/cm^2) increased only when preincubated with all-*trans* retinal (12 μM). (*B*) The mean amplitude of the current density at +80 mV significantly increased when HEMs were incubated with 9-*cis* or all-*trans* retinal and stimulated with UVR (240 mJ/cm^2), but not in the absence of retinal. I_{UVR} = (5.29 ± 0.95) pA/pF for all-*trans* retinal and (6.54 ± 1.06) pA/pF for 9-*cis* retinal vs. (0.02 ± 0.09) pA/pF in the absence of retinal. n = 5–10 cells per condition, $P < 0.0005$, bars represent average ± SEM. (*C*) Current density was measured with a voltage step protocol in response to 240 mJ/cm^2 UVR following incubation with 9-*cis* or all-*trans* retinal (12 μM); +80 mV was used for measuring the UVR-induced current under various conditions. (*D*) Representative whole-cell currents recorded at +80 mV from HEMs stimulated with increasing doses of UVR: I, 40 mJ/cm^2 (20 mW/cm^2 for 2 s); II, 140 mJ/cm^2 (20 mW/cm^2 for 7 s); III, 240 mJ/cm^2 (20 mW/cm^2 for 12 s); and IV, 340 mJ/cm^2 (20 mW/cm^2 for 17 s). The increase in current evoked by 340 mJ/cm^2 UVR was blocked by RR (10 μM) (IV). The mean current density in response to 340 mJ/cm^2 was significantly decreased in the presence of RR (10 μM). n = 4–5 cells per condition, ± SEM. (*E*) The amplitude of the UVR-induced (240 mJ/cm^2) whole-cell current density in HEMs is dose-dependent. The current density of HEMs exposed to the UVR doses indicated in *D* were averaged for each dose, and the dose–response curve fit with a sigmoidal function. (*F*) The light-activated current in HEMs is UVA-specific. Mean amplitude of the increase in current density in HEMs stimulated with 250 mJ/cm^2 UVR (~90% UVA and ~10% UVB), the UVB component (280–320 nm, 25 mJ/cm^2), the UVA component (320–400 nm, 225 mJ/cm^2), 250 mJ/cm^2 blue (435–460 nm), or green (500–550 nm) light. UVA elicited a change in current density comparable to total UVR and much higher than UVB, blue or green. I_{UVR} = (5.13 ± 0.48) pA/pF, I_{UVA} = (4.85 ± 1.47) pA/pF, I_{blue} = (0.34 ± 0.28) pA/pF, I_{green} = (0.19 ± 0.05) pA/pF. n = 5–6 cells per condition, $P < 0.0001$ for UVR vs. UVB, blue or green, ± SEM.

(Fig. 1*D*), suggesting that ion channels at the plasma membrane mediate the UVR dose-dependent increase in whole-cell current. Upon exposure to UVR, the current started increasing after a short latency (1.00 ± 0.12 s) and began to decrease shortly after the UVR stimulus ceased. The time constants for the UVR-induced increase in current and its return to baseline were measured by monitoring the current over a longer time period using a pulse protocol (Fig. S1*A*) to optimize cell health during continuous UVR exposure at +80 mV. At 340 mJ/cm^2 UVR, the current reached steady-state with a time constant τ_{on} of 13.2 ± 2.9 s (n = 4) and decreased with a highly variable τ_{off} that ranged from 8.5 to 35.6 s (n = 4) (Fig. S1 *B* and *C*). Thus, exposure to physiological UVR doses elicits a retinal-dependent increase in ionic current in HEMs that has a time course consistent with activation of a transduction cascade and may involve a TRP channel.

UVR-Induced Current Is UVA-Specific. Is this photocurrent specific to UVR or does it occur across a wider range of light frequencies? We measured the spectral sensitivity of the retinal-dependent photocurrent in HEMs and found that light-induced changes in whole-cell currents in response to equal doses (250 mJ/cm^2) of UVR, blue or green light were significant only in response to UVR (Fig. 1*F*), suggesting that the photocurrent is UVR-specific. Solar UVR at the Earth's surface is comprised of ~95% UVA (320–400 nm) and ~5% UVB (280–320 nm) (21) and human skin elicits different responses to the two types of UVR. Although UVB exposure results in a delayed pigmentation response that occurs many hours to days later (22), brief UVA exposure leads to a rapid and transient response within minutes via a largely unknown mechanism (23, 24). Because UVA penetrates skin more deeply than UVB, HEMs, located in the basal layer of the epidermis, are exposed to significantly more UVA than UVB (25, 26). Because our UVR-stimulation source contains ~90% UVA and ~10% UVB, we compared the photocurrent amplitude in response to 250 mJ/cm^2 UVR to the components 25 mJ/cm^2 UVB or 225 mJ/cm^2 UVA. UVA evoked a photocurrent equal to that evoked by UVR but UVB-induced photocurrent was ≤ 5% of UVR-induced current (Fig. 1*F*).

TRPA1 Mediates the UVR-Induced Photocurrent in HEMs. We next sought to identify candidate ion channels for the UVR photocurrent. Because TRP channels are nonselective cation channels involved in many sensory signaling pathways (7), and TRPA1 is expressed in skin (14) and has a current-voltage relationship similar to the UVR photocurrent (Fig. 1*C*), we tested whether TRPA1 mediates the UVR photocurrent. TRPA1 is activated by numerous noxious compounds, pungent chemicals, and GPCRs (27–31), and was recently implicated in an extraocular UVR phototransduction system mediating light avoidance responses in *Drosophila* larvae (32).

We first investigated whether TRPA1 antagonists could reduce the UVR-evoked photocurrent. Whole-cell currents measured at +80 mV in HEMs increased as expected in response to 240 mJ/cm^2 UVR in the presence of the vehicle control (0.5% DMSO), but not in the presence of the broad TRP channel antagonist RR (10 μM), or the TRPA1 antagonists camphor (1 mM) (33, 34) and HC-030031 (100 μM) (27, 35) (Fig. 2*A*). The UVR photocurrent density was reduced by ~95% in the presence of RR, by ~93% with camphor, and by ~83% in the presence HC-030031 (Fig. 2*B*) at all voltages (Fig. 2*B*, *Inset*), indicating that TRPA1 is a viable candidate for mediating the photocurrent.

TRPA1 Expression Is Required for UVR-Induced Current in HEMs. To determine whether TRPA1 mRNA is endogenously present in HEMs, we used RT-PCR with TRPA1 specific primers. We amplified a band of the expected size (Fig. 2*C*), which was sequenced and found to correspond to human TRPA1 cDNA (NM_007332). To test that TRPA1 mRNA expression results in functional protein, we monitored whole-cell currents in HEMs in response to TRPA1 agonists and antagonists. Cinnamaldehyde (CA, 500 μM) evoked a significant increase in whole-cell current at +80 mV, which was blocked by treatment with 100 μM HC-030031 or 10 μM RR (Fig. 2 *D* and *E*), indicating that functional TRPA1 channels are present in HEMs.

To assess if TRPA1 expression directly correlates with UVR-induced photocurrent, we used TRPA1-targeted miRNA to reduce endogenous TRPA1 levels. HEMs expressing TRPA1-targeted

Downloaded at Palestinian Territory, occupied on December 18, 2021
www.manaraa.com

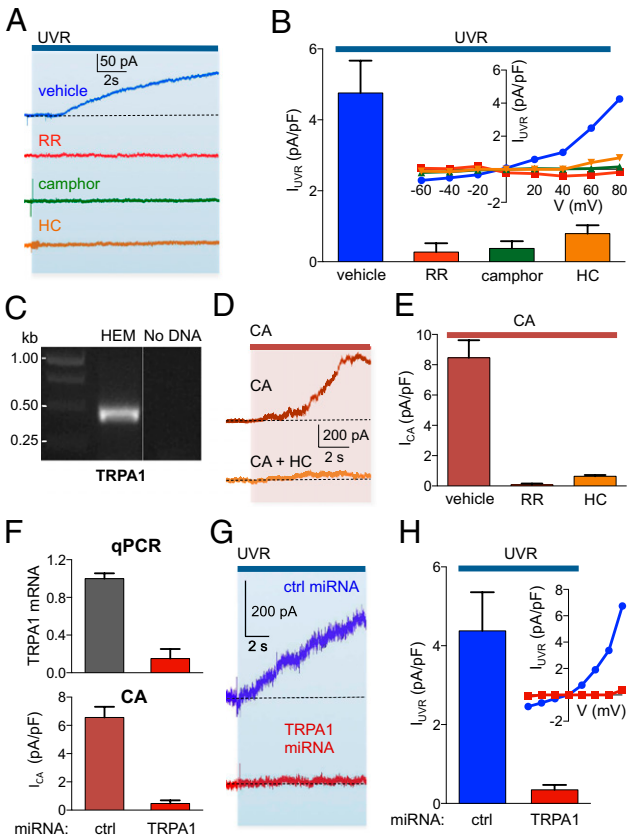

Fig. 2. TRPA1 is expressed in HEMs and mediates the UVR-induced current. (*A*) Representative retinal-dependent HEM whole-cell currents at +80 mV in response to 240 mJ/cm^2 UVR (20 mW/cm^2 for 12 s) were reduced by TRPA1 antagonists RR (10 μM), camphor (1 mM), or HC-030031 (100 μM) compared with vehicle (0.5% DMSO). (*B*) The UVR-induced (240 mJ/cm^2) increase in mean HEM whole-cell current density was significantly reduced by treatment with RR, camphor, or HC-030031 compared with vehicle. $I_{UVR} = (4.76 \pm 0.91)$ pA/pF, $I_{UVR/RR} = (0.27 \pm 0.25)$ pA/pF, $I_{UVR/camphor} = (0.36 \pm 0.20)$ pA/pF, $I_{UVR/HC\text{-}030031} = (0.79 \pm 0.24)$ pA/pF. n = 6–8 cells per condition, $P < 0.001$, ± SEM. (*Inset*) UVR-induced increases in HEM current density as a function of voltage, in the presence of vehicle, RR, camphor, or HC-030031. (*C*) TRPA1 mRNA is expressed in HEMs. RT-PCR using HEM cDNA and TRPA1 specific primers identified a DNA band of the expected size that was analyzed and found to correspond to human TRPA1 cDNA. (*D*) Functional TRPA1 channels are present in HEMs. HEM whole-cell current measured at +80 mV was increased by TRPA1 agonist CA (500 μM), but not by coapplication of CA and TRPA1 antagonist HC-030031 (100 μM). (*E*) The mean whole-cell current density of HEMs was significantly increased by CA, but not when coapplied with RR (10 μM) or HC-030031 (100 μM). $I_{CA} = (8.46 \pm 1.16)$ pA/pF, $I_{CA/RR} = (0.64 \pm 0.08)$ pA/pF, $I_{CA/HC\text{-}030031} = (0.08 \pm 0.08)$ pA/pF. n = 4–5 cells per condition, $P < 0.0007$, ± SEM. (*F*) HEMs expressing TRPA1-targeted miRNA have reduced levels of TRPA1 mRNA and current. (*Upper*) Quantitative PCR (qPCR) analysis showed an ∼85% reduction in TRPA1 mRNA levels in HEMs expressing TRPA1-targeted miRNA, compared with control miRNA. n = 3 experiments, $P < 0.002$, ± SEM. (*Lower*) Mean CA-evoked (500 μM) current density at +80 mV in HEMs expressing TRPA1-targeted miRNA was ∼93% lower compared with control miRNA. $I_{CA/ctrl\ miRNA} = (6.56 \pm 0.76)$ pA/pF, $I_{CA/TRPA1\ miRNA} = (0.47 \pm 0.22)$ pA/pF. n = 6 cells per condition, $P < 0.0001$, ± SEM. (*G*) Representative HEM expressing TRPA1-targeted miRNA exhibited a much smaller UVR-induced (240 mJ/cm^2) increase in current at +80 mV than a HEM expressing control miRNA. (*H*) HEMs expressing TRPA1-targeted miRNA had a ∼92% lower peak UVR photocurrent density compared with those expressing control miRNA. $I_{UVR/ctrl\ miRNA} = (4.66 \pm 0.86)$ pA/pF, $I_{UVR/TRPA1\ miRNA} = (0.35 \pm 0.12)$ pA/pF. n = 9–10 cells per condition, $P < 0.0001$, ± SEM (*Inset*) UVR-induced increase in current density vs. voltage in HEMs expressing control or TRPA1-targeted miRNA.

miRNA had TRPA1 mRNA levels ∼85% lower compared with control miRNA (Fig. 2*F*) and exhibited CA-evoked whole-cell currents ∼93% smaller than HEMs expressing control miRNA (Fig. 2*F*), suggesting that TRPA1-targeted miRNA expression resulted in reduced levels of TRPA1 mRNA as well as functional protein. We then measured changes in current in response to 240 mJ/cm^2 UVR in HEMs expressing TRPA1-targeted or control miRNA (Fig. 2*G*). We found that UVR-induced photocurrent was reduced by ∼92% in cells expressing TRPA1 miRNA compared with control miRNA (Fig. 2*H*), at all voltages (Fig. 2*H*, *Inset*), suggesting that TRPA1 expression is required for the photocurrent.

TRPA1 Is Activated Downstream of a G Protein- and PLC-Dependent Signaling Cascade. How does UVR activate TRPA1 in HEMs? UVA has been shown to activate a Ca^{2+}-permeable current, albeit irreversibly, at UVA doses ∼100-times higher than in our system, and with a different voltage dependence (36). Exposure to UVA leads to generation of reactive oxygen species (ROS), which activate TRPA1 expressed in human embryonic kidney 293 (HEK293) cells (37), which can be mimicked by exposure to 1 mM hydrogen peroxide (H_2O_2) and reduced by the antioxidant dithiothreital (DTT, 10 mM) (37). To test whether ROS mediate UVR-induced activation of TRPA1 in HEMs, we applied concentrations of H_2O_2 (150 μM) that generate ROS levels similar to those generated by our UVR doses (38) and found no significant increase in HEM whole-cell currents (Fig. S2 *A* and *B*). In addition, DTT (10 mM) did not significantly alter UVR photocurrent (Fig. S2 *A* and *B*) or Ca^{2+} responses (Fig. S2 *C* and *D*). We conclude that ROS do not mediate TRPA1 activation in HEMs exposed to low UVR doses, although ROS may be relevant at higher UVR doses.

To test if UVR activates TRPA1 directly or through a signaling pathway specific to HEMs, we expressed TRPA1 in Chinese hamster ovary K1 (CHO-K1) cells and measured whole-cell currents elicited by CA (500 μM) or 240 mJ/cm^2 UVR. CA evoked an outwardly rectifying current in CHO-K1 cells expressing TRPA1, but not in untransfected cells. UVR, however, did not significantly increase the current in CHO-K1 cells expressing TRPA1 or untransfected, regardless of preincubation with retinal (Fig. 3 *A*–*C*). These results show that UVR-activation of TRPA1 is indirect and specific to HEMs.

Light is detected in the retina by opsin GPCRs and TRP channels can be activated downstream: TRPs contribute to melanopsin-activated phototransduction in intrinsically photosensitive retinal ganglion cells (8, 9, 11), and also mediate the light-sensitive ionic conductance in *Drosophila* phototransduction (3–5). As UVR activates TRPA1 in a retinal-dependent manner and retinal is the chromophore required for opsin activation, we investigated if UVR activates TRPA1 downstream of an opsin-mediated G protein signaling cascade by blocking G protein activation with either guanosine 5′-O-2-thiodiphosphate (GDPβS) or suramin (39–41). In HEMs dialyzed with GDPβS (1 mM) or suramin (50 μM), UVR failed to induce a significant current (Fig. 3 *D* and *E*), suggesting that the photocurrent requires G protein signaling. We also examined if G protein-mediated activation of PLCβ is required for the UVR photocurrent. Treatment with the PLC inhibitor U73122 (9 μM) (42) significantly reduced the retinal-dependent UVR photocurrent at all voltages compared with its inactive analog U73343 (9 μM) (Fig. 3 *F*–*H*). These results indicate an extraocular UVR phototransduction cascade in human melanocytes leads to TRPA1 activation through G protein signaling and PLC activation.

We recently characterized a retinal-dependent UVR-activated pathway in HEMs that leads to a rapid increase in intracellular Ca^{2+} concentration ($[Ca^{2+}]_{ic}$) (15). Because TRPA1 can be regulated by $[Ca^{2+}]_{ic}$ (43, 44), we tested if the increase in $[Ca^{2+}]_{ic}$ contributes to TRPA1 activation by measuring the retinal-dependent photocurrent in response to 240 mJ/cm^2 UVR in HEMs dialyzed with the Ca^{2+} buffers EGTA or BAPTA [1,2-bis(*o*-aminophenoxy)ethane-N,N,N′,N′-tetraacetic acid] for ∼3 min. Similar responses were measured in HEMs dialyzed with 10 mM EGTA to prevent UVR-induced changes in $[Ca^{2+}]_{ic}$ and 20 μM EGTA to allow for an increase in $[Ca^{2+}]_{ic}$ (Fig. S3 *A* and *B*).

Downloaded at Palestinian Territory, occupied on December 18, 2021
www.manaraa.com

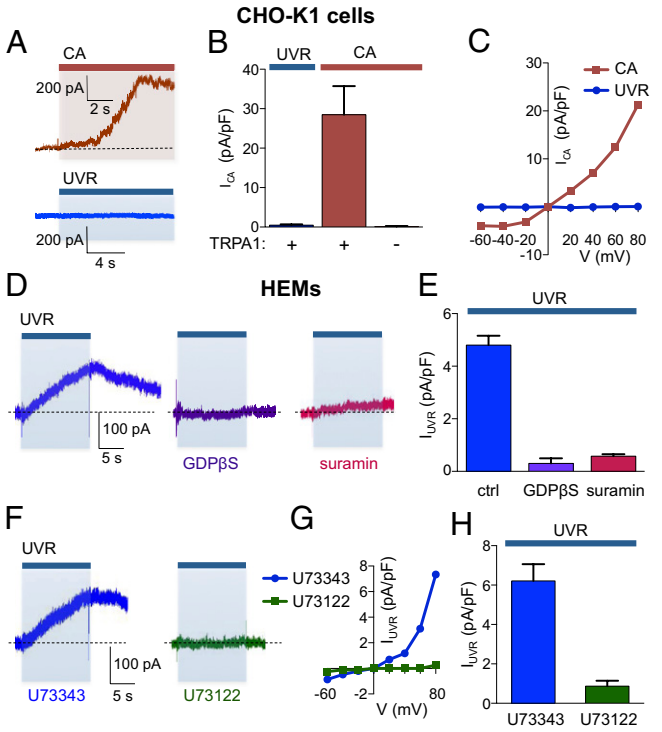

Fig. 3. TRPA1 is activated downstream of a G protein and PLC-dependent signaling cascade. (*A*) TRPA1 expressed in CHO-K1 cells did not exhibit UVR- and retinal-dependent current. Whole-cell currents at +80 mV from representative CHO-K1 cells expressing TRPA1 were increased by 500 μM CA (*Upper* trace), but not by 240 mJ/cm^2 UVR (*Lower* trace) following incubation with all-*trans* retinal. (*B*) The mean whole-cell current density in CHO-K1 cells increased significantly only in cells expressing TRPA1 and stimulated with CA, but not in cells expressing TRPA1, incubated with all-*trans* retinal, and stimulated with 240 mJ/cm^2 UVR. $I_{TRPA1/UVR+retinal}$ = (0.46 ± 0.24) pA/pF, $I_{TRPA1/CA}$ = (28.48 ± 7.27) pA/pF, $I_{ω/CA}$ = (0.09 ± 0.17) pA/pF. n = 4–5 cells per condition, $P < 0.008$, ± SEM. (*C*) The CA-activated current in CHO-K1 cells expressing TRPA1 has a voltage-dependence similar to that of the UVR-induced current in HEMs (Fig. 1*C*). Stimulation of CHO-K1 cells expressing TRPA1 and incubated with all-*trans* retinal with 240 mJ/cm^2 UVR did not evoke a current at any voltage. (*D*) The UVR-activated current is G protein-dependent. The UVR-induced (240 mJ/cm^2) increase in currents at +80 mV in representative HEMs was abolished by intracellular GDPβS (1 mM) and by suramin (50 μM). (*E*) The UVR-induced (240 mJ/cm^2) increase in mean HEM whole-cell current density was significantly reduced by dialyzing cells with 1 mM GDPβS or 50 μM suramin. I_{UVR} = (4.80 ± 0.36) pA/pF, $I_{UVR/GDPβS}$ = (0.30 ± 0.20) pA/pF, $I_{UVR/suramin}$ = (0.58 ± 0.07) pA/pF. n = 6–7 cells per condition, $P <$ 0.0001, ± SEM. (*F*) The UVR-activated current is PLC-dependent. The UVR-induced (240 mJ/cm^2) increase in representative HEM whole-cell currents at +80 mV was abolished in the presence of the PLC inhibitor U73122 (9 μM), but not its inactive analog U73343 (9 μM). (*G*) UVR-induced increases in HEM current density as a function of voltage, in the presence of U73122 (9 μM) or its inactive analog U73343 (9 μM). (*H*) The UVR-induced (240 mJ/cm^2) increase in mean HEM whole-cell current density was significantly reduced by treatment with U73122 (9 μM) compared with its inactive analog U73343 (9 μM). $I_{UVR/U73122}$ = (6.21 ± 0.85) pA/pF, $I_{UVR/U73343}$ = (0.86 ± 0.28) pA/pF. n = 5–6 cells per condition, $P < 0.0002$, ± SEM.

Because the effect of increased $[Ca^{2+}]_{ic}$ on TRPA1 could be local, we also measured the UVR-induced current in the presence of intracellular BAPTA (10 mM), and observed no significant difference (Fig. S3 *A* and *B*). These results suggest that the UVR-induced activation of TRPA1 is independent of the Ca^{2+} release that occurs in HEMs.

TRPA1 Contributes to UVR-Induced Calcium Responses. Our data suggest the UVR-induced, retinal-dependent, and G protein-mediated activation of TRPA1 is not caused by the Ca^{2+} release triggered by the same stimulus (15). It is more likely that in response to UVR, the calcium release and the TRPA1-mediated calcium influx are branches of the same pathway and both contribute to intracellular Ca^{2+} elevation. We investigated the contribution of the UVR photocurrent to the UVR-induced retinal-dependent increase in $[Ca^{2+}]_{ic}$, by monitoring intracellular Ca^{2+} in HEMs using the fluorometric Ca^{2+} indicator Fluo-4. To distinguish between Ca^{2+} influx and Ca^{2+} release, we compared the retinal-dependent Ca^{2+} responses elicited by UVR in the presence or absence of extracellular Ca^{2+} (+$[Ca^{2+}]_{ec}$ vs. −$[Ca^{2+}]_{ec}$) (Fig. 4*A*). Paired experiments showed that, despite variations in the cellular responses evoked in individual experiments, UVR induced a significantly greater Ca^{2+} response in the presence of $[Ca^{2+}]_{ec}$ (Fig. 4 *B* and *C*). The initial slope of the Ca^{2+} response (during the first 20 s) was also decreased by ∼52% in the absence of $[Ca^{2+}]_{ec}$, suggesting that Ca^{2+} influx contributes to both the amplitude and kinetics of the UVR-induced Ca^{2+} response. We previously did not detect a difference in amplitude (figure 2 in ref. 15) because we did not account for the variability in cellular responses by using paired experiments as we do now (Fig. 4*C*). Furthermore, we previously used a data analysis method that did not take into account cells with minimal Ca^{2+} responses, which are more prevalent in the absence of $[Ca^{2+}]_{ec}$.

Does TRPA1, a Ca^{2+} permeable ion channel, account for the UVR-activated Ca^{2+} influx? To determine the contribution of TRPA1 activation to changes in $[Ca^{2+}]_{ic}$, we measured Ca^{2+} responses in HEMs preincubated with 100 μM HC-030031 and stimulated with UVR in the presence of $[Ca^{2+}]_{ec}$. Ca^{2+} responses were reduced by ∼57% by treatment with HC-030031 and were comparable to responses measured in the absence of $[Ca^{2+}]_{ec}$ (Fig. 4 *D* and *E*). To determine if the influx-independent portion of the UVR-induced Ca^{2+} response originates from intracellular stores, HEMs were preincubated with thapsigargin (1 μM) in the absence of $[Ca^{2+}]_{ec}$, which completely abolished retinal-dependent UVR-induced Ca^{2+} responses (Fig. 4 *D* and *E*), suggesting the elevation in $[Ca^{2+}]_{ic}$ is the results of both TRPA1-mediated Ca^{2+} influx and Ca^{2+} release from thapsigargin-sensitive stores. We next investigated whether TRPA1 expression is necessary for retinal-dependent UVR-induced Ca^{2+} influx in HEMs. Ca^{2+} responses in cells expressing TRPA1-targeted miRNA were reduced by ∼58% compared with HEMs expressing control miRNA (Fig. 4 *F* and *G*). These results demonstrate TRPA1 expression is required for retinal-dependent UVR-induced Ca^{2+} influx, which contributes significantly to the UVR-induced intracellular Ca^{2+} response in HEMs.

TRPA1 Is Required for UVR-Induced Early Melanin Synthesis. We have recently shown that in HEMs UVR induces a retinal- and Ca^{2+}-dependent increase in cellular melanin concentration within hours of exposure (15). This early melanin synthesis occurs on a much faster time scale than previously described pathways (45) and is Ca^{2+}-dependent (15). Because UVR-induced TRPA1 activation contributes to increases in intracellular free Ca^{2+}, we sought to determine whether TRPA1 activation is required for early melanin synthesis. We exposed HEMs to a UVR dose that results in a measurable increase in melanin (2.5 J/cm^2, corresponding to ∼40 min of UVR exposure in full sun) and quantified retinal-dependent changes in cellular melanin 8 h after UVR exposure relative to those measured in HEMs preincubated with retinal or preincubated with retinal and HC-030031, but not exposed to UVR. UVR exposure led to an ∼1.8-fold increase in melanin in untreated HEMs (vehicle) that was reduced by ∼80% in HEMs pretreated with the specific TRPA1 inhibitor HC-030031 (100 μM) (Fig. 5*A*), suggesting that UVR-induced activation of TRPA1 contributes to early melanin synthesis.

To determine the contribution of TRPA1-mediated influx to Ca^{2+} responses at UVR doses used to elicit an increase in melanin, we measured retinal-dependent Ca^{2+} responses induced by 2.5 J/cm^2 UVR. We found that exposure of HEMs to higher UVR doses elicited a Ca^{2+} response that remained elevated for a longer period, consistent with our previous results

Downloaded at Palestinian Territory, occupied on December 18, 2021
www.manaraa.com

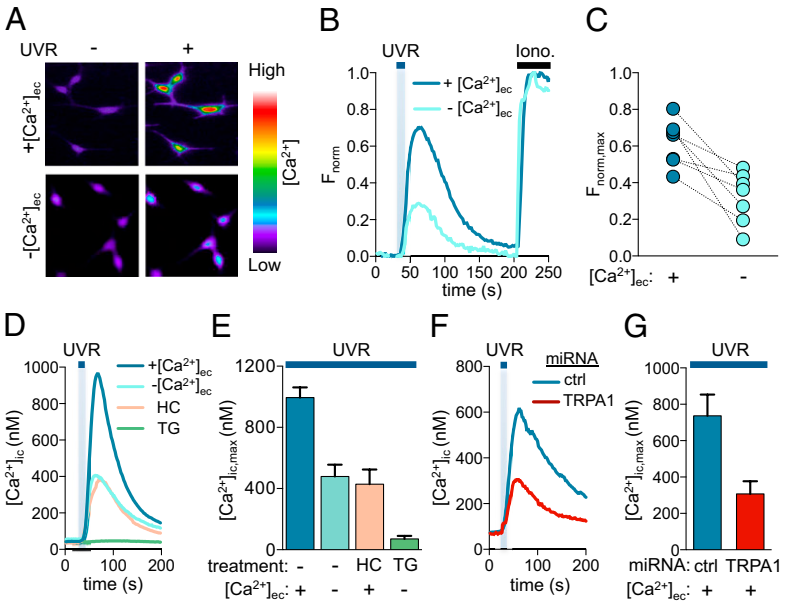

Fig. 4. TRPA1 contributes to UVR-induced calcium responses. (*A*) Pseudochrome Fluo-4 fluorescence images of HEMs preincubated with all-*trans* retinal and stimulated with 240 mJ/cm^2 UVR. (*Upper*) Images recorded in the presence of extracellular Ca^{2+} (+$[Ca^{2+}]_{ec}$), before UVR stimulation (−UVR) and at the peak UVR-induced Ca^{2+} response (+UVR). (*Lower*) Images recorded in the absence of extracellular Ca^{2+} (−$[Ca^{2+}]_{ec}$) and had a reduced response to UVR (*Upper* vs. *Lower* +UVR). (*B*) Representative Ca^{2+} imaging traces of HEMs preincubated with all-*trans* retinal and stimulated with UVR (240 mJ/cm^2). The peak fluorescence intensity normalized to ionomycin (2 μM) (F_{norm}) was higher in the presence of extracellular Ca^{2+} (+$[Ca^{2+}]_{ec}$) than in Ca^{2+}-free solution (−$[Ca^{2+}]_{ec}$). Each trace is the average of 10–12 cells from one experiment. (*C*) In paired experiments, the normalized peak fluorescence of Ca^{2+} responses ($F_{norm,\ max}$) of HEMs stimulated with 240 mJ/cm^2 UVR in the presence of extracellular Ca^{2+} (+$[Ca^{2+}]_{ec}$) was higher than in the absence of extracellular Ca^{2+} (−$[Ca^{2+}]_{ec}$). $F_{norm,max}$ = (0.62 ± 0.04) for +$[Ca^{2+}]_{ec}$, $F_{norm,max}$ = (0.33 ± 0.05) for −$[Ca^{2+}]_{ec}$. n = 8 experiments per condition; each experiment is the average of 8–15 cells, $P < 0.002$. (*D*) The apparent free intracellular Ca^{2+} concentration ($[Ca^{2+}]_{ic}$) of representative UVR-evoked (240 mJ/cm^2) retinal-dependent responses in the presence of extracellular Ca^{2+} (+$[Ca^{2+}]_{ec}$) was similarly reduced by HC-030031 (100 μM) and the absence of extracellular Ca^{2+} (−$[Ca^{2+}]_{ec}$). Incubation with thapsigargin (1 μM) in the absence of extracellular Ca^{2+} abolished UVR-induced Ca^{2+} responses. (*E*) The mean increase in apparent free $[Ca^{2+}]_{ic}$ in response to 240 mJ/cm^2 UVR in the presence of extracellular Ca^{2+} (+$[Ca^{2+}]_{ec}$) was reduced by ∼52% in the absence of extracellular Ca^{2+} (−$[Ca^{2+}]_{ec}$), by ∼57% in the presence 100 μM HC-030031, and by ∼93% following pretreatment with 1 μM thapsigargin in the absence of extracellular Ca^{2+}. $[Ca^{2+}]_{ic,max}$ = (994 ± 67) nM for +$[Ca^{2+}]_{ec}$, (479 ± 78) nM for −$[Ca^{2+}]_{ec}$, (429 ± 96) nM for HC-030031, (71 ± 21) nM for thapsigargin. n = 6–8 experiments per condition, $P \leq 0.003$, ± SEM. (*F*) HEMs expressing TRPA1-targeted miRNA had a reduced retinal-dependent Ca^{2+} response to UVR (240 mJ/cm^2), compared with HEMs expressing control miRNA, both stimulated in the presence of extracellular Ca^{2+}. n = 4–8 cells per condition. (*G*) The mean peak increase in apparent free $[Ca^{2+}]_{ic}$ (nM) induced by 240 mJ/cm^2 UVR in HEMs expressing TRPA1-targeted miRNA was reduced by ∼58% compared with control miRNA. $[Ca^{2+}]_{ic,max}$ = (737 ± 117) nM for control, (307 ± 70) nM for TRPA1-targeted miRNA. n = 5 experiments per condition, $P < 0.001$, ± SEM.

(15). Treatment with HC-030031 (100 μM) decreased the peak amplitude of the Ca^{2+} response and reduced the sustained elevation by a greater extent (Fig. 5*B*). Taken together with our previous data suggesting that the sustained Ca^{2+} response is important for UVR-induced early melanin synthesis (15), these results indicate that TRPA1 activation is required to maintain the sustained $[Ca^{2+}]_{ic}$ response necessary for changes in cellular melanin.

We next investigated whether expression of TRPA1 is necessary for UVR-induced early melanin synthesis in HEMs. HEMs expressing control or TRPA1-targeted miRNA were stimulated with 2.5 J/cm^2 UVR and relative melanin increases were quantified 8 h after exposure. Remarkably, retinal-dependent changes in cellular melanin were abolished in cells expressing TRPA1 miRNA compared with control miRNA (Fig. 5*C*). These results suggest that TRPA1 is essential for retinal-dependent UVR-induced early melanin synthesis. Thus, TRPA1 function is critical for a unique UVR phototransduction pathway in human melanocytes that leads to early melanin synthesis.

Conclusion

The ability to detect and respond to light stimuli is critical for survival. Human eyes do so using photoreceptors that transduce visible light into electrical signals to mediate visual and nonvisual processes (10). We have shown that human skin also has the ability to detect and respond to UV light using a phototransduction mechanism in melanocytes (15). We now demonstrate that TRPA1 is critical for UVA signaling in human skin cells and provide evidence that a retinal-dependent G protein cascade activates TRPA1 ion channels in a unique extraocular phototransduction pathway. Activation of this pathway leads to early melanin synthesis, thus allowing for rapid UVR detection and response in human melanocytes (Fig. S4). Our results suggest that UVR activation of a TRPA1 conductance may have an important protective skin function in response to damaging UVR.

Materials and Methods

Human Melanocyte Culture. Primary HEMs from neonatal foreskin (Cascade Biologics/Life Technologies) were cultured in Medium 254 and Human Melanocyte Growth Supplement (HMGS2; Cascade Biologics/Life Technologies) and propagated for ≤15 population doublings. Cells were cultured on glass

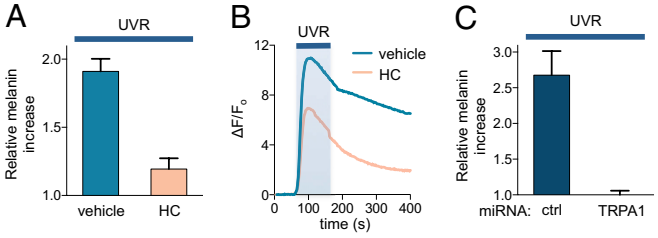

Fig. 5. TRPA1 is required for UVR-induced early melanin synthesis. (*A*) The UVR-induced retinal-dependent increase in melanin was reduced by 78.7 ± 12.5% in HEMs exposed to 2.5 J/cm^2 UVR in the presence of 100 μM HC-030031 compared with vehicle control (0.5% DMSO). Relative melanin increase measured 8 h after UVR exposure of HEMs preincubated with all-*trans* retinal, and calculated relative to melanin increase in cells receiving identical treatment without exposure to UVR. n = 12 experiments, $P < 0.0001$, ± SEM. (*B*) The retinal-dependent UVR-induced peak Ca^{2+} response in HEMs stimulated with 2.5 J/cm^2 UVR (20 mW/cm^2 for 125 s) in the presence of HC-030031 (100 μM) was reduced by ∼36.7%, but the sustained elevation measured 275 s after UVR stimulation was reduced by ∼70%. $n \geq 25$ cells per condition, $P < 0.007$ for differences in peak Ca^{2+} response and $P < 0.02$ for differences in sustained Ca^{2+} elevation for n = 6 experiments. (*C*) The retinal-dependent increase in melanin in response to 2.5 J/cm^2 UVR measured 8 h after exposure was abolished in HEMs expressing TRPA1-targeted miRNA compared with control miRNA. The melanin increase was calculated relative to changes in melanin measured in nonirradiated cells preincubated with retinal and expressing the corresponding miRNA. n = 6 experiments per condition, $P < 0.0007$, ± SEM.

Downloaded at Palestinian Territory, occupied on December 18, 2021

www.manaraa.com

coverslips for Ca^{2+} imaging and electrophysiology and on Petri dishes for all other experiments.

Light Stimulation. UVR stimulation was performed as previously described (15), using a Mercury-Xenon Arc lamp (Newport) with filtered output comparable to solar UVR. Each 1-s experimental irradiance of 10 mW/cm^2 equates to ~10 s exposure to bright solar UVR. Light was filtered as described in *SI Materials and Methods*. Physiological doses were applied by varying pulse power or duration.

Electrophysiology. Modified Ringer's extracellular solution contained: 150 mM NaCl, 1.8 mM $CaCl_2$, 1.2 mM $MgCl_2$, 10 mM D-glucose, 25 mM Hepes; pH 7.4, 310 mOsm/L. Unless stated otherwise, the internal pipette solution contained: 140 mM CsCl, 1 mM $MgCl_2$, 4 mM MgATP, 10 mM EGTA, 10 mM Hepes; pH 7.2, 290 mOsm/L. Whole-cell patch-clamp recordings were carried out at room temperature using an EPC 10 amplifier (HEKA Instruments) with PatchMaster software (HEKA Instruments), filtered at 2.9 kHz and digitized at 10 kHz.

Calcium Imaging. HEMs were incubated in the dark for 20 min in extracellular solution with 2 μM Fluo-4 AM (Life Technologies) and 250 μM sulfinpyrazone to prevent loss of Fluo-4 from cells, then for 20 min with 12 μM all-*trans* retinal, and transferred to the imaging chamber. Fluorescence images were acquired every 2 s using MetaMorph software (Molecular Devices) and analyzed as described in *SI Materials and Methods*. Cells were irradiated with UVR during time-lapse acquisition.

Melanin Quantification. Melanin was quantified as previously described (15) and briefly explained in *SI Materials and Methods*.

Statistical Analysis. Numerical data are mean ± SEM and P values were calculated using paired or unpaired two-tailed Student t test and considered significant when $P < 0.05$. n refers to the number of cells for electrophysiology experiments and the number of independent experiments for Ca^{2+} imaging and melanin quantification.

ACKNOWLEDGMENTS. We thank Dr. Joris Vriens and Dr. Ardem Patapoutian for providing the transient receptor potential A1-GFP construct, members of the E.O. laboratory for technical assistance, and Dr. Julie Kauer for critical reading of the manuscript. This work was supported in part by grants from Brown University (to E.O.); National Institutes of Health Training Grant T32 - GM077995; and a National Science Foundation Graduate Research Fellowship (to N.W.B.).

1. Lin JY, Fisher DE (2007) Melanocyte biology and skin pigmentation. *Nature* 445(7130): 843–850.
2. Kobayashi N, et al. (1998) Supranuclear melanin caps reduce ultraviolet induced DNA photoproducts in human epidermis. *J Invest Dermatol* 110(5):806–810.
3. Cosens DJ, Manning A (1969) Abnormal electroretinogram from a *Drosophila* mutant. *Nature* 224(5216):285–287.
4. Montell C, Jones K, Hafen E, Rubin G (1985) Rescue of the *Drosophila* phototransduction mutation trp by germline transformation. *Science* 230(4729):1040–1043.
5. Hardie RC, Minke B (1992) The trp gene is essential for a light-activated Ca2+ channel in *Drosophila* photoreceptors. *Neuron* 8(4):643–651.
6. Clapham DE (2003) TRP channels as cellular sensors. *Nature* 426(6966):517–524.
7. Damann N, Voets T, Nilius B (2008) TRPs in our senses. *Curr Biol* 18(18):R880–R889.
8. Berson DM, Dunn FA, Takao M (2002) Phototransduction by retinal ganglion cells that set the circadian clock. *Science* 295(5557):1070–1073.
9. Panda S, et al. (2005) Illumination of the melanopsin signaling pathway. *Science* 307(5709):600–604.
10. Yau KW, Hardie RC (2009) Phototransduction motifs and variations. *Cell* 139(2): 246–264.
11. Xue T, et al. (2011) Melanopsin signalling in mammalian iris and retina. *Nature* 479(7371):67–73.
12. Caterina MJ, et al. (2000) Impaired nociception and pain sensation in mice lacking the capsaicin receptor. *Science* 288(5464):306–313.
13. Denda M, Nakatani M, Ikeyama K, Tsutsumi M, Denda S (2007) Epidermal keratinocytes as the forefront of the sensory system. *Exp Dermatol* 16(3):157–161.
14. Atoyan R, Shander D, Botchkareva NV (2009) Non-neuronal expression of transient receptor potential type A1 (TRPA1) in human skin. *J Invest Dermatol* 129(9): 2312–2315.
15. Wicks NL, Chan JW, Najera JA, Ciriello JM, Oancea E (2011) UVA phototransduction drives early melanin synthesis in human melanocytes. *Curr Biol* 21(22):1906–1911.
16. Terakita A (2005) The opsins. *Genome Biol* 6(3):213.
17. Fan J, Rohrer B, Moiseyev G, Ma JX, Crouch RK (2003) Isorhodopsin rather than rhodopsin mediates rod function in RPE65 knock-out mice. *Proc Natl Acad Sci USA* 100(23):13662–13667.
18. Wu LJ, Sweet TB, Clapham DE (2010) International Union of Basic and Clinical Pharmacology. LXXVI. Current progress in the mammalian TRP ion channel family. *Pharmacol Rev* 62(3):381–404.
19. Hinterhuber G, et al. (2004) RPE65 of retinal pigment epithelium, a putative receptor molecule for plasma retinol-binding protein, is expressed in human keratinocytes. *J Invest Dermatol* 122(2):406–413.
20. Fu Y, et al. (2005) Intrinsically photosensitive retinal ganglion cells detect light with a vitamin A-based photopigment, melanopsin. *Proc Natl Acad Sci USA* 102(29): 10339–10344.
21. Narayanan DL, Saladi RN, Fox JL (2010) Ultraviolet radiation and skin cancer. *Int J Dermatol* 49(9):978–986.
22. Choi W, et al. (2010) Regulation of human skin pigmentation in situ by repetitive UV exposure: Molecular characterization of responses to UVA and/or UVB. *J Invest Dermatol* 130(6):1685–1696.
23. Jimbow K, Pathak MA, Fitzpatrick TB (1973) Effect of ultraviolet on the distribution pattern of microfilaments and microtubules and on the nucleus in human melanocytes. *Yale J Biol Med* 46(5):411–426.
24. Routaboul C, Denis A, Vinche A (1999) Immediate pigment darkening: Description, kinetic and biological function. *Eur J Dermatol* 9(2):95–99.
25. Halliday GM, Cadet J (2012) It's all about position: The basal layer of human epidermis is particularly susceptible to different types of sunlight-induced DNA damage. *J Invest Dermatol* 132(2):265–267.
26. Duval C, Regnier M, Schmidt R (2001) Distinct melanogenic response of human melanocytes in mono-culture, in co-culture with keratinocytes and in reconstructed epidermis, to UV exposure. *Pigment Cell Res* 14(5):348–355.
27. Bandell M, et al. (2004) Noxious cold ion channel TRPA1 is activated by pungent compounds and bradykinin. *Neuron* 41(6):849–857.
28. Jordt SE, et al. (2004) Mustard oils and cannabinoids excite sensory nerve fibres through the TRP channel ANKTM1. *Nature* 427(6971):260–265.
29. Macpherson LJ, et al. (2007) Noxious compounds activate TRPA1 ion channels through covalent modification of cysteines. *Nature* 445(7127):541–545.
30. Sawada Y, Hosokawa H, Matsumura K, Kobayashi S (2008) Activation of transient receptor potential ankyrin 1 by hydrogen peroxide. *Eur J Neurosci* 27(5):1131–1142.
31. Wilson SR, et al. (2011) TRPA1 is required for histamine-independent, Mas-related G protein-coupled receptor-mediated itch. *Nat Neurosci* 14(5):595–602.
32. Xiang Y, et al. (2010) Light-avoidance-mediating photoreceptors tile the Drosophila larval body wall. *Nature* 468(7326):921–926.
33. Xu H, Blair NT, Clapham DE (2005) Camphor activates and strongly desensitizes the transient receptor potential vanilloid subtype 1 channel in a vanilloid-independent mechanism. *J Neurosci* 25(39):8924–8937.
34. Macpherson LJ, et al. (2006) More than cool: Promiscuous relationships of menthol and other sensory compounds. *Mol Cell Neurosci* 32(4):335–343.
35. McNamara CR, et al. (2007) TRPA1 mediates formalin-induced pain. *Proc Natl Acad Sci USA* 104(33):13525–13530.
36. Mendez F, Penner R (1998) Near-visible ultraviolet light induces a novel ubiquitous calcium-permeable cation current in mammalian cell lines. *J Physiol* 507(Pt 2):365–377.
37. Hill K, Schaefer M (2009) Ultraviolet light and photosensitising agents activate TRPA1 via generation of oxidative stress. *Cell Calcium* 45(2):155–164.
38. Linetsky M, Ortwerth BJ (1996) Quantitation of the reactive oxygen species generated by the UVA irradiation of ascorbic acid-glycated lens proteins. *Photochem Photobiol* 63(5):649–655.
39. Eckstein F, Cassel D, Levkovitz H, Lowe M, Selinger Z (1979) Guanosine 5′-O-(2-thiodiphosphate). An inhibitor of adenylate cyclase stimulation by guanine nucleotides and fluoride ions. *J Biol Chem* 254(19):9829–9834.
40. Chung WC, Kermode JC (2005) Suramin disrupts receptor-G protein coupling by blocking association of G protein alpha and betagamma subunits. *J Pharmacol Exp Ther* 313(1):191–198.
41. Freissmuth M, et al. (1996) Suramin analogues as subtype-selective G protein inhibitors. *Mol Pharmacol* 49(4):602–611.
42. Bleasdale JE, et al. (1989) Inhibition of phospholipase C dependent processes by U-73, 122. *Adv Prostaglandin Thromboxane Leukot Res* 19:590–593.
43. Doerner JF, Gisselmann G, Hatt H, Wetzel CH (2007) Transient receptor potential channel A1 is directly gated by calcium ions. *J Biol Chem* 282(18):13180–13189.
44. Zurborg S, Yurgionas B, Jira JA, Caspani O, Heppenstall PA (2007) Direct activation of the ion channel TRPA1 by Ca2+. *Nat Neurosci* 10(3):277–279.
45. Cui R, et al. (2007) Central role of p53 in the suntan response and pathologic hyperpigmentation. *Cell* 128(5):853–864.

Downloaded at Palestinian Territory, occupied on December 18, 2021

www.manaraa.com